EFFECT OF THE ADIPONECTIN SIGNALING PATHWAY ON PLASMA MEMBRANE ORDER

An Undergraduate Research Scholars Thesis

by

KYUNG HO JUNG

Submitted to the Undergraduate Research Scholars program at
Texas A&M University
in partial fulfillment of the requirements for the designation as an

UNDERGRADUATE RESEARCH SCHOLAR

Approved by Research Advisor: Dr. Robert S. Chapkin

May 2020

Major: Biochemistry

TABLE OF CONTENTS

ABSTRACT

Effect of the Adiponectin Signaling Pathway on Plasma Membrane Order

Kyung Ho Jung
Department of Biochemistry and Biophysics
Texas A&M University

Research Advisor: Dr. Robert S. Chapkin
Department of Nutrition
Texas A&M University

Cancer is the second leading cause of death in the world. It is responsible for 16% of death around the world, making it a major health concern in the 21th Century. Approximately, 18.1 million people were diagnosed with cancer in 2018 alone and the numbers are projected to increase even further. Among the major types of cancer, colorectal cancer is the third most prevalent and deadliest cancer type. It is promising to note that up to 75% of colorectal cancer cases could be prevented with dietary modifications, lifestyle changes, and regular screening. Due to the highly preventative nature of the disease, it is critical to understand the mechanisms behind colorectal cancer initiation and proliferation. Adiponectin is an adipose tissue-derived adipokine, whose levels are inversely related to colorectal cancer. With the consensus in the literature that obesity results in low circulating levels of adiponectin, a cancer risk factor, it is pertinent to determine the mechanism by which adiponectin signals through its respective receptors to affect cancer initiation. Recently, our lab showed that AdipoRon, a small-molecule adiponectin receptor agonist, reduces plasma membrane order in a cholesterol-dependent manner. Because cholesterol makes up almost 30% of the total lipids present in the plasma membrane, its structural role and homeostasis is essential for proper signaling through the

plasma membrane. Because the plasma membrane serves as a nexus integrating intracellular components that enable various fundamental cellular signaling, including cell proliferations, we hypothesized that AdipoRon signals through AdipoR1 and AdipoR2 to initiate cholesterol mobilization from the plasma membrane, causing a decrease in membrane order. Moreover, we hypothesized that disrupting adiponectin signaling through knocking out AdipoR1 and AdipoR2 would result in an increase in plasma membrane order. Here, we demonstrate that AdipoRon decreases membrane order in a dose-dependent manner in WT HAP1 cells. Moreover, using both confocal imaging and imaging flow cytometry, we show that disrupting adiponectin signaling by knocking out either individual or both adiponectin receptors changes the order of the plasma membrane. These findings are noteworthy because they may in part explain how adiponectin protects against colorectal cancer in part by altering plasma membrane order.

CHAPTER I

INTRODUCTION

Cancer is the second leading cause of death in the world. It is responsible for 16% of death around the world, making it a major health concern in the 21th Century. Approximately, 18.1 million people were diagnosed with cancer in 2018 alone and the numbers are projected to increase even further. Among the major types of cancer, colorectal cancer is the third most prevalent as well as the third deadliest cancer type (1). It is promising to note that up to 75% of colorectal cancer cases could be prevented with dietary modifications, lifestyle changes, and regular screening (2). Due to the highly preventative nature of this disease, it is critical to understand the mechanisms behind colorectal cancer initiation and proliferation. The plasma membrane of cells serves as a nexus integrating intracellular components that enable various fundamental cellular signaling, including networks that regulate cell proliferation. Many studies have observed that alterations in the biophysical properties of the plasma membrane correlate with obesity-linked inflammation, metabolic disorders, altered T cell responses, and cell proliferation (3-5). With regard to colorectal cancer, our lab has previously shown that recombinant adiponectin and AdipoRon treatment reduces $Lgr5^{+}$ stem cell number in colonic organoid cultures from healthy mice (6). With the consensus in literature that obesity results in low circulating levels of adiponectin, it is pertinent to determine the mechanism by which receptor-dependent adiponectin signaling (7-12) affects cancer initiation.

Adiponectin is an adipocytokine with a molecular mass of approximately 30kDa that is produced and secreted by the adipose tissue (13-16). Circulating in plasma, adiponectin exists predominantly in three major forms: trimer, hexamer, high molecular weight (HMW) multimer

(17-20) as well as a globular form in which the N-terminal tail is proteolytically cleaved (21,22). Circulating levels of adiponectin in non-obese individuals range from 3 to 30 μg/mL while obese individuals tend to exhibit a significant reduction in these levels (23). Because of its association with colorectal cancer and obesity in general (6), understanding adiponectin signaling is crucial in developing therapeutic strategies for the future.

Adiponectin predominantly signals through two major receptors, adiponectin receptor 1 (AdipoR1) and adiponectin receptor 2 (AdipoR2). These receptors are comprised of seven alpha-helices that span the transmembrane region of the plasma membrane, similar to G protein-coupled receptors (GPCRs). However, unlike GPCRs, the N-termini of AdipoR1 and AdipoR2 are oriented within the cytoplasm of the cell and the C-terminal tails reside in the extracellular region (24). Congruent with low circulating level of adiponectin in obese individuals, AdipoR1 and AdipoR2 expression is lower in obese individuals (25,26). Based on the proposed crystal structures of AdipoR1 and AdipoR2, AdipoRon, a synthetic orally active small-molecule AdipoR agonist was discovered and utilized in various experiments to illustrate its protection against obesity related diseases, inflammation, atherosclerosis, and other diseases (27). In order to study the importance of AdipoR1 and AdipoR2 in adiponectin signaling, we utilized an isogenic cell culture model with single and double knockouts of each adiponectin receptor to modulate adiponectin-dependent signaling.

Recently, our lab showed that AdipoRon reduces plasma membrane order in a cholesterol dependent manner (28). The plasma membrane is composed of a bilayer of lipids and incorporated proteins, whose interactions are critical in order to propagate signals correctly from the extracellular region to the cytoplasm of the cell (29). Because cholesterol makes up almost 30% of the total lipids present in the plasma membrane, its structural role and homeostasis is

essential for proper signaling through the plasma membrane (30). From this information, we hypothesized that AdipoRon signals through AdipoR1 and AdipoR2 to initiate cholesterol mobilization from the plasma membrane, causing a decrease in membrane order. Moreover, we hypothesized that disrupting adiponectin signaling through knocking out AdipoR1 and AdipoR2 would result in an increase in plasma membrane order. Here, we demonstrate that AdipoRon decreases membrane order in a dose-dependent manner in WT HAP1 cells. Moreover, using both confocal imaging and imaging flow cytometry, we show that disrupting adiponectin signaling by knocking out either individual or both adiponectin receptors changes actin polymerization, cholesterol level in PM, ultimately affecting the order of the plasma membrane.

CHAPTER II

METHODS

Cell culture

HAP1 is a near-haploid human cell line that was derived from the male chronic myelogenous leukemia cell line KBM-7 (31). HAP1 cells (passages 6-18) were cultured under regulated conditions; 37℃ and 5% CO2 in Iscove's Modified Dulbecco's Medium (IMDM) (LifeTech 12440-053), supplemented with 10% fetal bovine serum (HyClone SH300084.03), and 1% Penicillin/Streptomycin (LifeTech 15140-122). HAP1 cell lines were passaged every 2 to 3 days when ~75% confluency was obtained. HAP1 AdipoR1 KO and HAP1 AdipoR2 KO cell lines were generated via CRISPR/Cas9-editing and were purchased from Horizon Discovery, Ltd. Genomic DNA analysis was performed to validate CRISPR effectively knocked out AdipoR1 and AdipoR2 individually in HAP1 cell line (**Fig.S1**). HAP1 AdipoR1 and AdipoR2 double knockouts were generated in our lab via CRISPR/Cas9 editing in HAP1 AdipoR2 KO cells with a guide RNA directed toward exon 6 of AdipoR1. These cell lines were treated with 0, 1, 5, 10, 20 μM AdipoRon or a vehicle control, 0.1% dimethyl sulfoxide (DMSO) for 24 hours. In addition, some cultures were incubated with 5mM or 10mM methyl- β-cyclodextrin (MβCD) for 30 min to deplete cholesterol from the plasma membrane as we have previously described (32).

Giant plasma membrane vesicles (GPMV) generation and isolation

GPMVs are rafts taken directly form the plasma membrane and only contains the lipid bilayers and the embedded membrane proteins (33). Because they don't contain other biological components of the cell, it is an excellent model system to study the plasma membrane (34). Cells

were plated on 24 well plates and incubated at 37℃ with 5% CO_2 for 24 h. Cells were then treated with either different concentrations of AdipoRon or 0.1% DMSO for 24 h. GPMVs were subsequently generated by washing each well with DPBS, followed by GPMV buffer (10 mM HEPES, 100 mM NaCl, 2mM CaCl2) (35). Vesiculation buffer (50 mM PFA, 2mM DTT, and GPMV buffer) was added for at least 4 h at 37℃. The solution with GPMVs from each well was transferred to a 1.7 mL tube and centrifuged at 100 X g for 2 min to remove excess cell debris. The resultant GPMVs were either immediately used or stored at 4℃ for use the following day.

Measuring membrane order in cells via confocal microscopy

Cells were plated in an eight-chamber cell-culture treated imaging plate (Eppendorf 0030742028) and incubated at 37℃ with 5% CO_2 for 24 h. Cells were then treated with either different concentrations of AdipoRon or 0.1% DMSO for 24 h. Prior to confocal microscopy, media was removed and cells were washed once with live cell imaging solution (LCIS) (Invitrogen #A14291DJ) and fresh LCIS was added to each well. 5μM Di-4-ANEPPDHQ (Di4) was added directly to each well. Imaging was performed on a Leica DMi8 confocal microscope immediately after addition of Di4 to prevent internalization of the dye. Cells were imaged with a 1.15 NA 40x plan Apochromat oil objective. A 488nm laser was used to excite Di4, and emission wavelengths were collected in two channels representing ordered (O: 500-580 nm) and disordered (D: 620-700 nm). Generalized polarization (GP) was calculated using the equation below. Where G is a calibration factor determined using a solution of 500 μM Di4 in DMSO following a procedure previously described (36).

Generalized polarization equation:

$$GP = \frac{(Intensity\ (O) - \left(G\ \times\ Intensity\ (D)\right))}{(Intensity\ (O) + \left(G\ \times\ Intensity\ (D)\right))}$$

Measuring membrane order in GPMVs via imaging flow cytometry

Imaging flow cytometry was performed via Amnis FlowSight. An aliquot (49 μL) of isolated GPMVs were pipetted into a non-stick 1.7 mL tube (Phenix, MH-815SA). To specifically observe plasma membrane order, Di4 dye was chosen for its low internalization property (37). A 1 μL aliquot of 50 μM Di4 was added to the 49 μL of sample GPMVs to ultimately make a 1 μM final concentration of the Di4 dye. The sample vial was held at room temperature for 5 min prior to data collection of the sample. A 488 nm laser was used to excite Di4, and emission wavelengths were collected in two preset channels representing ordered (O: 480-560 nm) and disordered (D: 640-745 nm). Due to the inability to acquire a calibration image using this equipment, the G factor was omitted, and GP was calculated as stated above using Amnis IDEAS software.

Measuring actin polymerization

Cells were plated in an eight-chamber cell-culture treated imaging slide (Eppendorf 0030742028) and incubated at 37℃ with 5% CO_2 for 24 h. Staining solution consisting of 1:1000 CellMask Green Plasma Membrane Stain (Invitrogen #C37608), 1μM SiR-actin (Cytoskeleton #Cy-SC001), 5μg/mL Hoechst 3342 (Invitrogen #H3570), and live cell imaging solution (Invitrogen #A14291DJ) was warmed to 37℃ before use. Cells were washed with live cell imaging solution then incubated with staining solution at 37℃ for 30 min.

Lipid extraction from GPMVs

Cells were grown in a T-75 flask until 75% confluency was obtained. Cells were washed with DPBS, followed by GPMV buffer. Vesiculation buffer (50 mM PFA, 2mM DTT, and GPMV buffer) was added for at least 4 h at 37℃. GPMVs were harvested and centrifuged at 100 x g for 2 min at 4℃. Afterwards, the supernatant containing GPMVs were transferred to

low-retention 1.7 mL tubes, which were then centrifuged at 20,000 x g for 60 min at 4°C. Supernatant was removed and the pellet was resuspended in 200 µL of methanol for each tube and transferred to a 15 mL glass tube with a teflon screw cap. 2 mL of $CHCl_3$ and 0.6 mL of cold 0.1 KCl was added and vortexed for 1 min. Samples were centrifuged at 2000 x g for 5 min at 4°C. The lower phase was transferred to another 4 mL glass vial. Extraction was performed twice per sample, pooled, dried using N_2 gas and re-dissolved in 1 mL of Folch (2:1, v/v, chloroform/methanol).

Phosphate Colorimetric Assay

A 50 µL aliquot of each lipid extraction was taken and added to the bottom of a 13 x 100 mm glass tube (VWR #47729-572 or Fisher #14-961-27). 30 µL of a 10% $Mg(NO_3)_2*6H_2O$ was added to the glass tube and gently mixed. Samples were dried using N_2 gas. Individual tubes were held over a flame for 30 seconds. 100 µL of 1N HCl were added to dissolve the sample, and 400 µL of dH_2O was added to the sample mix. Phosphate Colorimetric Assay Kit (BioVision, K410) was used to measure phosphate levels in GPMVs. For this purpose, 200 µL of each sample was incubated with phosphate reagent in the dark for 30 minutes at room temperature. Absorbance was read at 650 nm using a plate reader.

Amplex Red Cholesterol Assay

Free and esterified cholesterol concentrations were determined using an Amplex Red Cholesterol Assay Kit (Invitrogen #A12216) according to the manufacturer's instructions. 100 µL were taken from 1mL $CHCl_3$ containing lipid extract was pipetted into a low-retention 0.65 mL tube. Each tube was dried and extracted under N_2 gas and re-dissolved in 210 µL of 1X reaction buffer from the kit. A working solution consisting of 300 µM Amplex red reagent containing 2 U/mL cholesterol oxidase and 0.2 U/mL cholesterol esterase was prepared for

measuring total cholesterol. No addition of cholesterol esterase prepared a working solution that measures only free cholesterol. 50 µL of samples, cholesterol standards, and positive controls were transferred to respective wells. 50 µL of total cholesterol working solution or free cholesterol working solution were added to respective wells. Samples were mixed gently and incubated in the dark at 37℃ for at least 30 min. Fluorescence was measured using a fluorescence microplate reader using excitation in the range of 530 – 560 nm and emission detection at 590 nm. For each point, background fluorescence was corrected by subtracting the values derived from the zero-cholesterol control.

Statistics

One-way analysis of variance (ANOVA) with Tukey's multiple comparisons test was used to assess statistical significance of the differences between means across experimental treatments. All data are presented as mean ± standard error of the mean (SEM). All analyses were performed using Prism 8 statistical software (GraphPad).

CHAPTER III

RESULTS AND DISCUSSION

Our lab previously observed that organoids treated with AdipoRon, a small molecule adiponectin receptor agonist, reduced $Lgr5^{+}$ stem cell numbers suggesting that modulation of this pathway may be beneficial in preventing the initiation of colorectal cancer (6). Our lab also demonstrated that treatment with AdipoRon attenuated Wnt signaling in 3T3 mouse fibroblasts containing a Wnt reporter (28). In addition, immortalized mouse colonocytes (YAMC cells) treated with AdipoRon, exhibited a decrease in membrane order presumably as a result of free-cholesterol depletion from the plasma membrane (28), indicating that AdipoRon may attenuate Wnt signaling by changing the biophysical properties of the plasma membrane. However, to date, there is no known mechanism to explain this phenomenon. We propose that AdipoRon specifically signals through the adiponectin receptors, AdipoR1 and AdipoR2, to modulate lipid content and thus the biophysical properties of the plasma membrane, which ultimately affects Wnt signaling. Here, we show that AdipoRon decreases plasma membrane order in a dose-dependent manner and establish a concentration at which AdipoRon elicits a response similar to a physiologically relevant dose of adiponectin. We also show that under basal conditions, AdipoR1 and AdipoR2 are integral to maintaining biophysical homeostasis within the plasma membrane.

AdipoRon decreases membrane order in a dose-dependent manner

Treatment of AdipoRon has been shown to decrease plasma membrane order in YAMC cells (28). This study utilized HAP1 cell lines due to the ease of genetic modification with this cell line. Before investigating the effects of any genetic manipulations, the effect of AdipoRon

on HAP1 WT cells was determined. For this purpose, HAP1 WT cells were seeded in a 24 well plate and incubated for 24 h. Cells were then treated with either 0, 1, 5, 10, or 20 μM of AdipoRon, 0.1% DMSO, or 10μg/mL adiponectin for 24 h. Physiologically relevant concentration of adiponectin between 3μg/mL and 30 μg/mL was chosen for the study. A 30-min treatment with either 5mM or 10mM MβCD was used as a positive control for detecting changes in membrane order, as MβCD removes cholesterol from the plasma membrane decreasing membrane order (32). Untreated wells served as a negative control. GPMVs, which are comprised solely of the plasma membrane (33) were then generated and Di-4-ANEPPDHQ (Di4) was used to measure order of the plasma membrane. Because AdipoRon was dissolved in DMSO, all data from AdipoRon treatments were normalized to the 0.1% DMSO treatment, while adiponectin treatments were normalized to untreated samples. Incubation with AdipoRon resulted in a dose-dependent decrease in membrane order in GPMVs (**Fig. 1**). It is also interesting to note that the 10 μM AdipoRon treatment induced a similar decrease in membrane order relative to the physiologically relevant 10μg/mL adiponectin treatment.

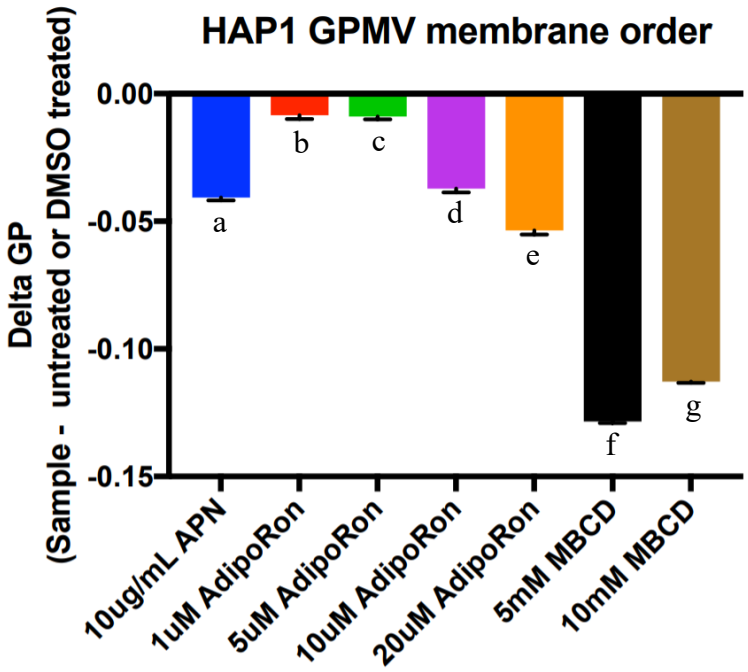

Figure 1. Plasma membrane order for HAP1 WT GPMVs decreases due to AdipoRon and adiponectin treatments. ΔGP (sample-vehicle) values indicate a dose-dependent decrease in plasma membrane order due to 24-hour AdipoRon treatment. Comparison between all means are $p<0.0001$ ($n>1500$ GPMVs).Adiponectin treatment values were normalized to untreated samples while AdipoRon treatment values were normalized to 0.1%DMSO values (Table S1)

AdipoRon signals specifically through AdipoR1 and AdipoR2 to modulate plasma membrane order

In order to determine the extent to which AdipoRon signals through AdipoR1 and AdipoR2 to modulate the biophysical properties of the plasma membrane, HAP1 cells lacking either AdipoR1, AdipoR2, or both receptors were treated with 10μM AdipoRon and membrane order was measured after 24 h. R1KO cells exhibited a decrease in membrane order while R2KO cells exhibited an increase in membrane order (**Fig. 2**), suggesting that, although the two receptors have additive effects under basal conditions, when stimulated AdipoR1 and AdipoR2 elicit opposing effects on membrane order. In agreement with our hypothesis, the AdipoR double knockout (R2R1KO) cells exhibited no significant change in membrane order as

compared to WT. These data indicate that AdipoRon modulates the biophysical properties of the plasma membrane via both AdipoR1 and AdipoR2.

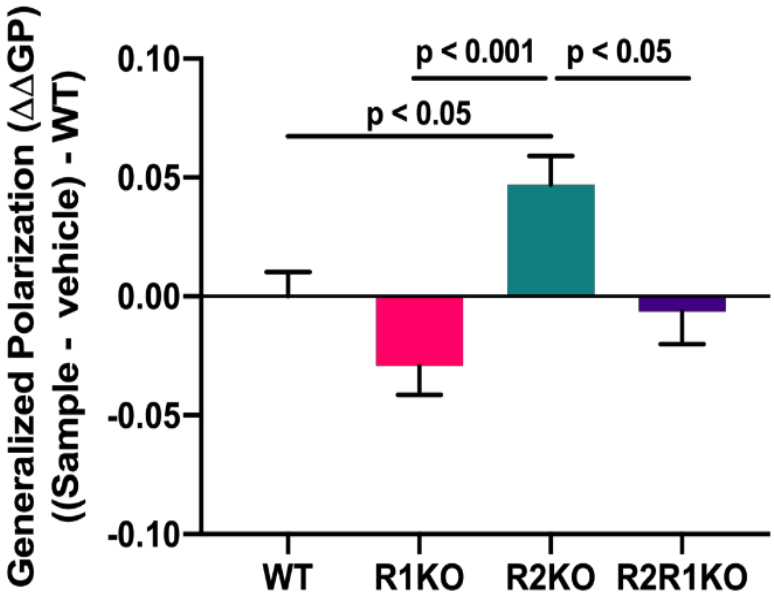

Figure 2. HAP1 whole cell confocal imaging comparing the effect of AdipoRon on plasma membrane order ΔΔGP ((sample-vehicle)-WT) values of HAP1 WT, AdipoR1 KO, AdipoR2 KO, and AdipoR2R1 double KO cells treated with 10 uM AdipoRon for 24 h (n = 9-10 fields of view). Values obtained can be seen in Table S2.

Disruption of AdipoR1 and AdipoR2 increases membrane order in intact cells

After confirming WT HAP1 GPMVs respond to AdipoRon in a similar manner as YAMC GPMVs (26), the effect of each adiponectin receptor on membrane order was investigated using single and double receptor knockout HAP1 cell lines—AdipoR1 KO (R1KO), AdipoR2 KO (R2KO), and AdipoR1/R2 KO (R2R1KO), respectively. Cells were imaged via confocal microscopy. R1KO and R2KO cells exhibited a similar increase in membrane order relative to WT, while R2R1KO cells had an increase in membrane order roughly double that of the single knockouts (**Fig. 3**). These data suggest that both adiponectin receptors are involved in homeostasis of plasma membrane order even in the absence of ligand. Moreover, the additive

increase in membrane order for the AdipoR double knockout cell line (R2R1KO) suggests that the two receptors have redundancy within the pathway.

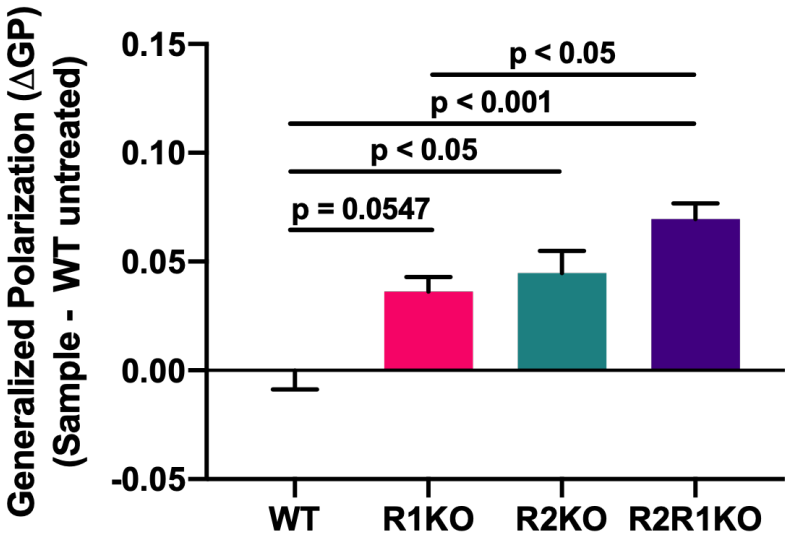

Figure 3. HAP1 whole cell confocal imaging comparing the effect of AdipoR knockout on plasma membrane order. ΔGP (sample -WT untreated) values of untreated HAP1 WT, AdipoR1 KO, AdipoR2 KO, and AdipoR2R1 double KO. (n = 5-10 fields of view). All values obtained can be found in Table S3.

Disruption of AdipoR1 and AdipoR2 decreases membrane order in GPMVs

Based on the increase in membrane order for intact cells, we hypothesized that GPMVs would show a similar trend for plasma membrane order. In order to observe the effect AdipoR1 and AdipoR2 has on the plasma membrane in the absence of the cytoskeleton, the experiment was repeated with the exception that GPMVs from each cell line were assayed using imaging flow cytometry. Contrary to observations made from intact cells, GPMVs from the single and double AdipoR KO cell lines exhibited a decrease in plasma membrane order relative to WT (**Fig. 4**). This is presumably due to the lack of a cytoskeleton, suggesting that the cytoskeleton may play a role in mediating both AdipoR1 and AdipoR2 effects on the plasma membrane.

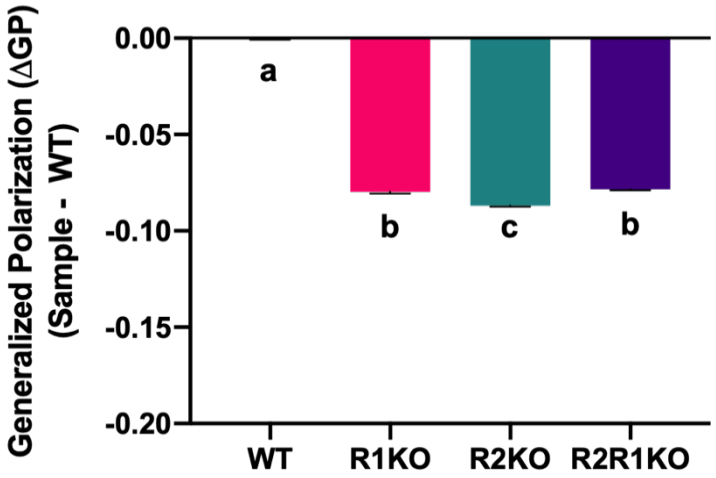

Figure 4. HAP1 GPMVs imaging using flow cytometry comparing the effect of AdipoR knockout on plasma membrane order. (A) ΔGP (sample -WT untreated) values of HAP1 WT, AdipoR1 KO, AdipoR2 KO, and AdipoR2R1 double KO illustrating the effect of the knockout itself on plasma membrane order. $p < 0.0001$ ($n > 4500$ GPMVs). Mean values used to generate the graph can be found in Table S4.

Disruption of AdipoR1 and AdipoR2 increases actin polymerization in intact cells

Because the main difference between intact cells and GPMVs is the cytoskeleton, which can also regulate plasma membrane order (38), the effect of disrupting adiponectin signaling on actin polymerization was studied. Cells were imaged via confocal microscopy using SiR-actin to assess actin polymerization (**Fig. S5**). While R1KO and R2KO exhibited no significant change compared to WT, AdipoR double knockout (R2R1KO) cells exhibited a significant increase in actin polymerization **(Fig. 5**). These data suggest that, under basal conditions, AdipoR1 and AdipoR2 have redundant properties, in maintaining normal actin polymerization.

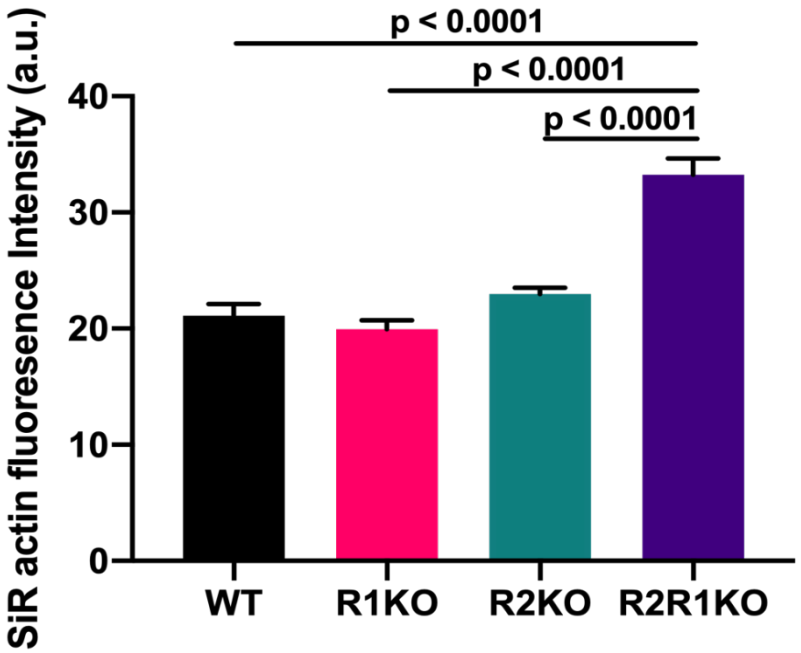

Figure 5. HAP1 whole cell confocal imaging comparing the effect of AdipoR knockout on actin polymerization. SiR actin fluorescence intensity values of untreated HAP1 WT, AdipoR1 KO, AdipoR2 KO, and AdipoR2R1 double KO (n=158-302 cells). Mean intensity values can be found in Table S5.

Disruption of AdipoR1 and AdipoR2 alters cholesterol level in PM

To determine the effect of disrupting adiponectin signaling on cholesterol level in the plasma membrane, lipid extraction of GPMVs, phosphate colorimetric assay, and Amplex red assay were performed. R2KO showed a decrease in cholesterol level while R2R1KO had a slight increase compared to HAP1 WT (**Fig 6**). This illustrates a potential role of AdipoR2 to regulate cholesterol localization in the plasma membrane.

R1KO exhibited increase in plasma membrane order even when no significant difference of actin polymerization and cholesterol levels compared to HAP1 WT was observed. This illustrates that there are various other factors besides cytoskeleton and cholesterol concentration that are altered following disruption of adiponectin signaling. Future investigations that look into

other changes such as lipid content of the plasma membrane are needed to further elucidate the mechanism by which adiponectin signaling modulates plasma membrane order.

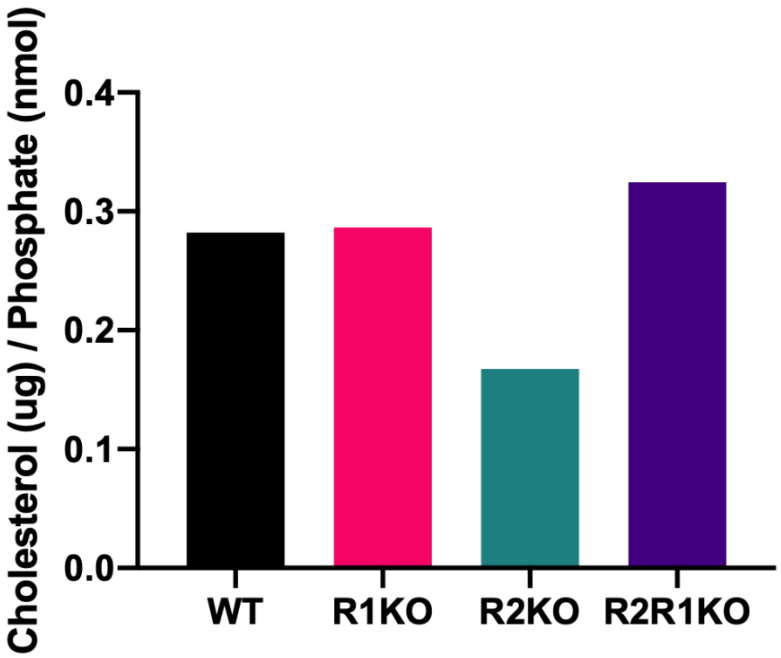

Figure 6. Free cholesterol decreases in the absence of adiponectin receptor 2. WT HAP1 cells, as well as lines lacking either AdipoR1, AdipoR2, or both receptors were grown in a T-175 flask to ~80 confluency. Giant plasma membrane vesicles (GPMVs) were generated and isolated. Lipids were extracted from GPMVs via Folch (2:1, v/v/, chloroform/methanol) method. Free cholesterol concentrations were determined using an Amplex Red Cholesterol Assay Kit. Cholesterol concentration was normalized to the phospholipid concentration using an inorganic phosphate assay. Results are from a single assay. Raw values obtained can be found in Table S6.

CHAPTER IV

CONCLUSION

In this study, we observed the effects of both activation and disruption of adiponectin signaling on the biophysical properties of the plasma membrane, e.g., membrane order, non-esterified cholesterol levels. Here, we show that AdipoRon induces a dose-dependent decrease in membrane order in HAP1 WT GPMVs. Membrane order in cell lines lacking either AdipoR1, AdipoR2, or both receptors were examined in the presence or absence of AdipoRon and compared to WT cells. Stimulation of adiponectin signaling via AdipoRon in whole cells decreased membrane order in R1KO cells while increasing order in R2KO cells. It is noteworthy, that no difference in membrane order was observed between the AdipoR double knockout and WT following exposure to AdipoRon, indicating that this adiponectin mimetic signals through AdipoR1 and AdipoR2 to modulate the biophysical properties of the plasma membrane. Additionally, disruption of adiponectin signaling via adiponectin receptor knockouts increased membrane order in intact cells, with AdipoR double knockout cells exhibiting a two-fold increase in membrane order. This suggests that, under basal conditions, AdipoR1 and AdipoR2 have redundant properties, affecting the plasma membrane in a similar manner.

Data from GPMVs, however, exhibited a substantial decrease in membrane order in all adiponectin receptor knockout cell lines, showing opposite trends compared to intact cells. Because GPMVs lack components of the cytoskeleton that are influential to the biophysical properties of the plasma membrane, the effect of adiponectin signaling on actin polymerization was examined. Our data showed that compared to WT, disrupting adiponectin signaling by knocking out both adiponectin receptors increased actin polymerization while there were no

significant differences in AdipoR single knockouts. This also suggests that, under basal conditions, AdipoR1 and AdipoR2 have redundant properties in maintaining normal actin polymerization (**Fig. 7**).

Perhaps most importantly, R1KO cells exhibited an increase in plasma membrane order even when no significant difference in actin polymerization and cholesterol levels compared to HAP1 WT was observed. This indicates that factors other than the cytoskeleton and or cholesterol content of the plasma membrane could be contributing to the changes in biophysical properties of the plasma membrane that are observed when adiponectin signaling is disrupted. One potential key contributor could be a change in the sphingolipid content of the plasma membrane (39,40). Future experiments that utilize mass spectrometry-based lipidomic are needed to further assess whether the concentration of other lipid populations is altered in the plasma membrane as a result of disrupted adiponectin signaling.

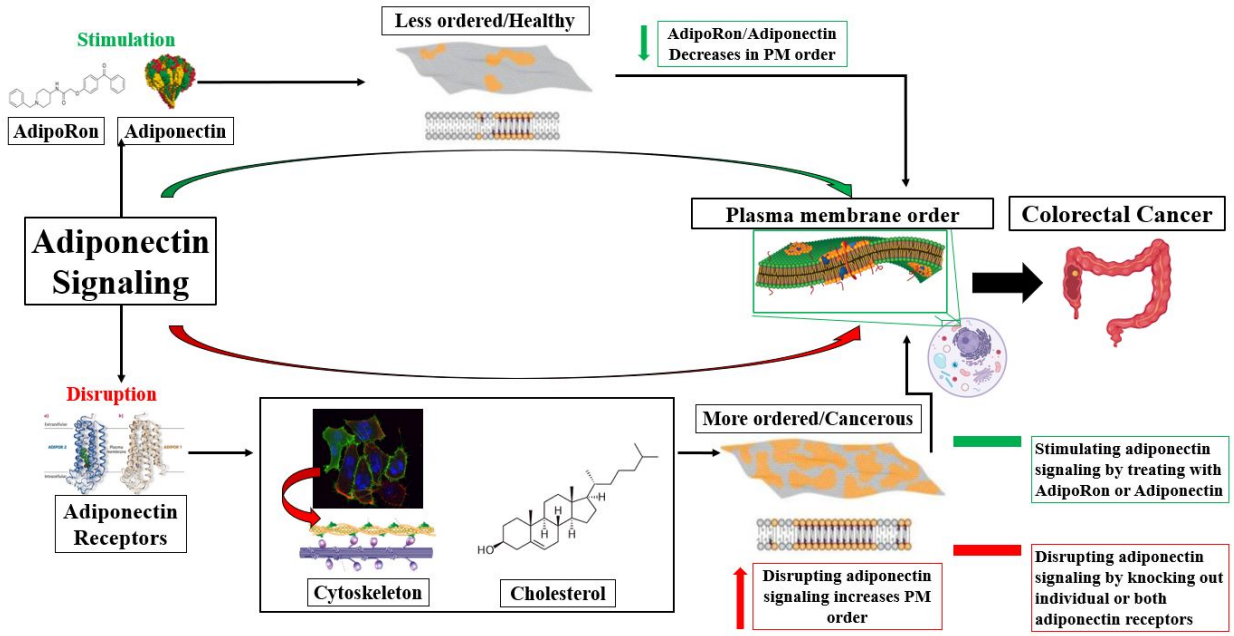

Figure 7 Summary diagram highlighting the effect of both stimulating and disrupting adiponectin signaling. AdipoRon and adiponectin treatment decreases membrane order in a dose-dependent manner. In comparison, disrupting adiponectin signaling by knocking out Adiponectin receptors increased membrane order and altered both actin polymerization and cholesterol levels in the plasma membrane.

Understanding the relationship between colorectal cancer risk and adiponectin signaling is a complex task. However, our data suggest that alterations in plasma membrane order via modulation of the adiponectin signaling pathway may serve as a source of future therapeutic approaches.

REFERENCES

1. Siegel, Rebecca L., et al. “Cancer Statistics, 2019.” *CA: A Cancer Journal for Clinicians*, vol. 69, no. 1, 2019, pp. 7–34., doi:10.3322/caac.21551.

2. Chan, Andrew T., and Edward L. Giovannucci. “Primary Prevention of Colorectal Cancer.” *Gastroenterology*, vol. 138, no. 6, 2010, doi:10.1053/j.gastro.2010.01.057.

3. Pollock, Abigail H., et al. “Prolonged Intake of Dietary Lipids Alters Membrane Structure and T Cell Responses in LDLr−/− Mice.” *The Journal of Immunology*, vol. 196, no. 10, 2016, pp. 3993–4002., doi:10.4049/jimmunol.1501261.

4. Gianfrancesco, Marco A., et al. “Lipid Bilayer Stress in Obesity-Linked Inflammatory and Metabolic Disorders.” *Biochemical Pharmacology*, vol. 153, 2018, pp. 168–183., doi:10.1016/j.bcp.2018.02.022.

5. Erazo-Oliveras, Alfredo, et al. “Functional Link between Plasma Membrane Spatiotemporal Dynamics, Cancer Biology, and Dietary Membrane-Altering Agents.” *Cancer and Metastasis Reviews*, vol. 37, no. 2-3, Feb. 2018, pp. 519–544., doi:10.1007/s10555-018-9733-1.

6. Declercq, V., et al. “Obesity Promotes Colonic Stem Cell Expansion during Cancer Initiation.” *Cancer Letters*, vol. 369, no. 2, 2015, pp. 336–343., doi:10.1016/j.canlet.2015.10.001.

7. Lu, Weiqun, et al. “Low Circulating Total Adiponectin, Especially Its Non-High-Molecular Weight Fraction, Represents a Promising Risk Factor for Colorectal Cancer: a Meta-Analysis.” *OncoTargets and Therapy*, Volume 11, 2018, pp. 2519–2531., doi:10.2147/ott.s157255.

8. Otake, Sayaka. “Decreased Levels of Plasma Adiponectin Associated with Increased Risk of Colorectal Cancer.” *World Journal of Gastroenterology*, vol. 16, no. 10, 2010, p. 1252., doi:10.3748/wjg.v16.i10.1252.

9. Karastergiou, Kalypso, and Vidya Mohamed-Ali. “The Autocrine and Paracrine Roles of Adipokines.” *Molecular and Cellular Endocrinology*, vol. 318, no. 1-2, 2010, pp. 69–78., doi:10.1016/j.mce.2009.11.011.

10. Okada-Iwabu, Miki, et al. “A Small-Molecule AdipoR Agonist for Type 2 Diabetes and Short Life in Obesity.” *Nature*, vol. 503, no. 7477, 2013, pp. 493–499., doi:10.1038/nature12656.

11. Stern, Jennifer H., et al. “Adiponectin, Leptin, and Fatty Acids in the Maintenance of Metabolic Homeostasis through Adipose Tissue Crosstalk.” *Cell Metabolism*, vol. 23, no. 5, 2016, pp. 770–784., doi:10.1016/j.cmet.2016.04.011.

12. Kim, A. Young, et al. “Adiponectin Represses Colon Cancer Cell Proliferation via AdipoR1- and -R2-Mediated AMPK Activation.” *The Journal of Clinical Endocrinology & Metabolism*, vol. 95, no. 5, 2010, pp. 2520–2520., doi:10.1210/jcem.95.5.9995.

13. Scherer, Philipp E., et al. “A Novel Serum Protein Similar to C1q, Produced Exclusively in Adipocytes.” *Journal of Biological Chemistry*, vol. 270, no. 45, Oct. 1995, pp. 26746–26749., doi:10.1074/jbc.270.45.26746.

14. Maeda, Kazuhisa. “Reprint of ‘CDNA Cloning and Expression of a Novel Adipose Specific Collagen-like Factor, apM1 (Dioseost Abundant Gene Transcript 1).’” *Biochemical and Biophysical Research Communications*, vol. 425, no. 3, 2012, pp. 556–559., doi:10.1016/j.bbrc.2012.08.023.

15. Nakano, Y., et al. “Isolation and Characterization of GBP28, a Novel Gelatin-Binding Protein Purified from Human Plasma.” *Journal of Biochemistry*, vol. 120, no. 4, Jan. 1996, pp. 803–812., doi:10.1093/oxfordjournals.jbchem.a021483.

16. Kadowaki, Takashi, and Toshimasa Yamauchi. “Adiponectin and Adiponectin Receptors.” *Endocrine Reviews*, vol. 26, no. 3, Jan. 2005, pp. 439–451., doi:10.1210/er.2005-0005.

17. Pajvani, Utpal B., et al. “Structure-Function Studies of the Adipocyte-Secreted Hormone Acrp30/Adiponectin.” *Journal of Biological Chemistry*, vol. 278, no. 11, 2002, pp. 9073–9085., doi:10.1074/jbc.m207198200.

18. Tsao, Tsu-Shuen, et al. “Oligomerization State-Dependent Activation of NF-KB Signaling Pathway by Adipocyte Complement-Related Protein of 30 KDa (Acrp30).” *Journal of Biological Chemistry*, vol. 277, no. 33, 2002, pp. 29359–29362., doi:10.1074/jbc.c200312200.

19. Waki, Hironori, et al. “Impaired Multimerization of Human Adiponectin Mutants Associated with Diabetes.” *Journal of Biological Chemistry*, vol. 278, no. 41, 2003, pp. 40352–40363., doi:10.1074/jbc.m300365200.

20. Qiang, L., et al. “Adiponectin Secretion Is Regulated by SIRT1 and the Endoplasmic Reticulum Oxidoreductase Ero1-L .” *Molecular and Cellular Biology*, vol. 27, no. 13, 2007, pp. 4698–4707., doi:10.1128/mcb.02279-06.

21. Fruebis, J., et al. “Proteolytic Cleavage Product of 30-KDa Adipocyte Complement-Related Protein Increases Fatty Acid Oxidation in Muscle and Causes Weight Loss in Mice.” *Proceedings of the National Academy of Sciences*, vol. 98, no. 4, 2001, pp. 2005–2010., doi:10.1073/pnas.98.4.2005.

22. Waki, Hironori, et al. “Generation of Globular Fragment of Adiponectin by Leukocyte Elastase Secreted by Monocytic Cell Line THP-1.” *Endocrinology*, vol. 146, no. 2, 2005, pp. 790–796., doi:10.1210/en.2004-1096.

23. Giannessi, D., et al. “Adiponectin Circulating Levels: A New Emerging Biomarker of Cardiovascular Risk.” *Pharmacological Research*, vol. 56, no. 6, 2007, pp. 459–467., doi:10.1016/j.phrs.2007.09.014.

24. Kadowaki, Takashi, and Toshimasa Yamauchi. “Adiponectin and Adiponectin Receptors.” *Endocrine Reviews*, vol. 26, no. 3, Jan. 2005, pp. 439–451., doi:10.1210/er.2005-0005.

25. Rasmussen, Maria S., et al. “Adiponectin Receptors in Human Adipose Tissue: Effects of Obesity, Weight Loss, and Fat Depots*.” *Obesity*, vol. 14, no. 1, 2006, pp. 28–35., doi:10.1038/oby.2006.5.

26. Nigro, Ersilia, et al. “New Insight into Adiponectin Role in Obesity and Obesity-Related Diseases.” *BioMed Research International*, vol. 2014, 2014, pp. 1–14., doi:10.1155/2014/658913.

27. Jr., A.m. Gotto. “Establishing the Benefit of Statins in Low-to-Moderate—Risk Primary Prevention: The Air Force/Texas Coronary Atherosclerosis Prevention Study (AFCAPS/TexCAPS).” *Atherosclerosis Supplements*, vol. 8, no. 2, 2007, pp. 3–8., doi:10.1016/j.atherosclerosissup.2007.02.002.

28. Salinas, Michael L., et al. “AdipoRon Attenuates Wnt Signaling by Reducing Cholesterol-Dependent Plasma Membrane Rigidity.” *Biophysical Journal*, vol. 118, no. 4, 2020, pp. 885–897., doi:10.1016/j.bpj.2019.09.009.

29. Grecco, Hernán E., et al. “Signaling from the Living Plasma Membrane.” *Cell*, vol. 144, no. 6, 2011, pp. 897–909., doi:10.1016/j.cell.2011.01.029.

30. Krause, Martin R., and Steven L. Regen. “The Structural Role of Cholesterol in Cell Membranes: From Condensed Bilayers to Lipid Rafts.” *Accounts of Chemical Research*, vol. 47, no. 12, 2014, pp. 3512–3521., doi:10.1021/ar500260t

31. Horizon Discovery Ltd. “HAP1 Knockout Cell Lines.” *,* 2015, horizondiscovery.com/en/products/gene-editing/cell-line-models/PIFs/Human-HAP1-Knockout-Cell-Lines.

32. Mahammad, Saleemulla, and Ingela Parmryd. “Cholesterol Depletion Using Methyl-β-Cyclodextrin.” *Methods in Molecular Biology Methods in Membrane Lipids*, 2014, pp. 91–102., doi:10.1007/978-1-4939-1752-5_8.

33. Chiang, Po-Chieh, et al. “Rupturing Giant Plasma Membrane Vesicles to Form Micron-Sized Supported Cell Plasma Membranes with Native Transmembrane Proteins.” *Nature News*, Nature Publishing Group, 9 Nov. 2017, www.nature.com/articles/s41598-017-15103-3.

34. Sezgin, Erdinc, et al. “Measuring Lipid Packing of Model and Cellular Membranes with Environment Sensitive Probes.” *Langmuir*, vol. 30, no. 27, 2014, pp. 8160–8166., doi:10.1021/la501226v.

35. Levental, K. R., and I. Levental. “Isolation of Giant Plasma Membrane Vesicles for Evaluation of Plasma Membrane Structure and Protein Partitioning.” *Methods in Molecular Biology Methods in Membrane Lipids*, 2014, pp. 65–77., doi:10.1007/978-1-4939-1752-5_6.

36. Levental, Kandice R., and Ilya Levental. “Giant Plasma Membrane Vesicles: Models for Understanding Membrane Organization.” *Lipid Domains Current Topics in Membranes*, 2015, pp. 25–57., doi:10.1016/bs.ctm.2015.03.009.

37. Sezgin, Erdinc, et al. “Elucidating Membrane Structure and Protein Behavior Using Giant Plasma Membrane Vesicles.” *Nature Protocols*, vol. 7, no. 6, Mar. 2012, pp. 1042–1051., doi:10.1038/nprot.2012.059.

38. Bezanilla, Magdalena, et al. “Cytoskeletal Dynamics: A View from the Membrane.” *Journal of Cell Biology*, vol. 209, no. 3, Nov. 2015, pp. 329–337., doi:10.1083/jcb.201502062.

39. Eich, Christina, et al. “Changes in Membrane Sphingolipid Composition Modulate Dynamics and Adhesion of Integrin Nanoclusters.” *Scientific Reports*, vol. 6, no. 1, 2016, doi:10.1038/srep20693.

40. Breslow, David K., and Jonathan S. Weissman. “Membranes in Balance: Mechanisms of Sphingolipid Homeostasis.” *Molecular Cell*, vol. 40, no. 2, 2010, pp. 267–279., doi:10.1016/j.molcel.2010.10.005.

SUPPLEMENTAL INFORMATION

Cell line validation

To validate each AdipoR single knockout cell lines, specific regions of DNA were analyzed. AdipoR1 KO is known to have a 5 bp deletion mutation at Exon 4 (12,031-12,035) while AdipoR2 KO is known to have a 5 bp deletion mutation at Exon 3 (81,845 – 81,849). To verify these 5 bp deletions, forward, sequence, and reverse primers were designed. Although standard primer design instructions were followed, such as more than 50% GC content, other features including binding affinity, hairpin formation, self-dimerization calculations were conducted via algorithms provided by the sequencing company GeneWiz. Annealing temperatures used for PCR were 54℃ for AdipoR1 and 60℃ for AdipoR2.

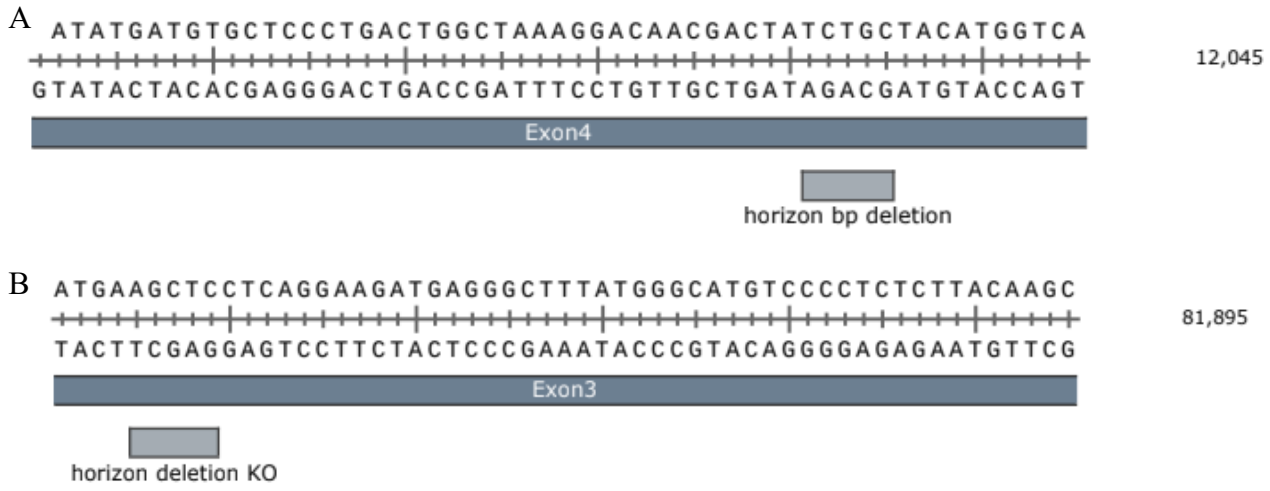

Figure S1. Five base pair deletion sites for individual adiponectin receptors. (A) Five base pair deletion for adiponectin receptor 1 located at Exon 4 (12,031 – 12,035). (B) Five base pair deletion for adiponectin receptor 2 located at Exon 3 (81,845 – 81,849).

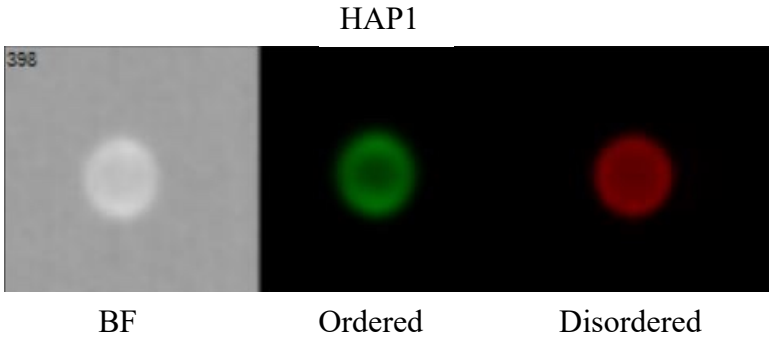

Figure S2. AdipoRon decreases membrane order in a dose-dependent manner. Representative FlowSight image of HAP1 cells stained with Di4. Starting from the left, Brightfield (BF), Ordered, and disordered images are shown.

Table S2. AdipoRon decreases membrane order in a dose-dependent manner raw data. Raw values of HAP1 WT treating with increasing concentration of AdipoRon.

Sample	Mean GP Value	SD	N
Untreated	-0.6016	0.0553	1669
0.1% DMSO	-0.5644	0.0591	1802
1uM AdipoRon	-0.5728	0.0646	1721
5uM AdipoRon	-0.5733	0.0536	2070
10uM AdipoRon	-0.6016	0.0643	2014
20uM AdipoRon	-0.618	0.0673	1805
10ug/mL APN	-0.6423	0.0452	1501
5mM MBCD	-0.7301	0.0246	1809
10mM MBCD	-0.7144	0.0246	2174

Table S3. HAP1 whole cell confocal imaging comparing the effect of AdipoRon on plasma membrane order. (A) Raw values of four cell lines when treated with 0.1% DMSO. (B) Raw values of four cell liens when treated with 10μM AdipoRon

A

WT	R1KO	R2KO	R2R1KO
-0.166	-0.138	-0.16	-0.133
-0.186	-0.173	-0.157	-0.13
-0.24	-0.155	-0.203	-0.13
-0.256	-0.155	-0.194	-0.177
-0.192	-0.167	-0.195	-0.192
-0.197	-0.198	-0.218	-0.185
-0.202	-0.198	-0.3	-0.169
-0.217	-0.218	-0.267	-0.17
-0.232	-0.223	-0.269	-0.207
-0.218	-0.226	-0.286	-0.204

B

WT	R1KO	R2KO	R2R1KO
-0.234	-0.23	-0.179	-0.182
-0.232	-0.269	-0.207	-0.199
-0.243	-0.256	-0.218	-0.175
-0.231	-0.262	-0.217	-0.201
-0.264	-0.251	-0.245	-0.237
-0.29	-0.299	-0.23	-0.251
-0.303	-0.265	-0.233	-0.28
-0.303	-0.273	-0.245	-0.293
-0.297	-0.359	-0.297	-0.263
-0.304		-0.303	-0.275

Table S4. HAP1 whole cell confocal imaging comparing the effect of AdipoR knockout on plasma membrane order. Raw values of HAP1 WT, R1KO, R2KO, R2R1KO untreated or treated with 0.1% DMSO, 10μM AdipoRon, or 5mM MBCD.

HAP1 WT

Untreated	DMSO	10uM AdipoRon	5mM MBCD
-0.212	-0.166	-0.234	-0.263
-0.253	-0.186	-0.232	-0.27
-0.209	-0.24	-0.243	-0.275
-0.209	-0.256	-0.231	-0.296
-0.235	-0.192	-0.264	-0.305
	-0.197	-0.29	-0.28
	-0.202	-0.303	-0.292
	-0.217	-0.303	-0.296
	-0.232	-0.297	-0.315
	-0.218	-0.304	-0.338

HAP1 R1KO

Untreated	0.1% DMSO	10uM AdipoRon	5mM MBCD
-0.174	-0.138	-0.23	-0.199
-0.194	-0.173	-0.269	-0.253
-0.161	-0.155	-0.256	-0.269
-0.162	-0.155	-0.262	-0.282
-0.17	-0.167	-0.251	-0.265
-0.208	-0.198	-0.299	-0.276
-0.159	-0.198	-0.265	-0.293
-0.208	-0.218	-0.273	-0.351
-0.209	-0.223	-0.359	-0.302
-0.21	-0.226		-0.305
-0.205			

HAP1 R2KO

Untreated	0.1% DMSO	10uM AdipoRon	5mM MBCD
-0.111	-0.16	-0.179	-0.24
-0.148	-0.157	-0.207	-0.252
-0.157	-0.203	-0.218	-0.314
-0.205	-0.194	-0.217	-0.424
-0.171	-0.195	-0.245	-0.379
-0.189	-0.218	-0.23	-0.337
-0.188	-0.3	-0.233	-0.347
-0.203	-0.267	-0.245	-0.344
-0.205	-0.269	-0.297	-0.335
-0.212	-0.286	-0.303	-0.338

HAP1 R2R1KO

Untreated	0.1% DMSO	10uM AdipoRon	5mM MBCD
-0.104	-0.133	-0.182	-0.217
-0.177	-0.13	-0.199	-0.233
-0.138	-0.13	-0.175	-0.211
-0.174	-0.177	-0.201	-0.277
-0.147	-0.192	-0.237	-0.222
-0.152	-0.185	-0.251	-0.396
-0.141	-0.169	-0.28	-0.339
-0.164	-0.17	-0.293	-0.334
-0.177	-0.207	-0.263	-0.361
-0.166	-0.204	-0.275	-0.34

Table S5. HAP1 GPMVs imaging using flow cytometry comparing the effect of AdipoR knockout on plasma membrane order. Raw values of HAP1 WT, R1KO, R2KO, R2R1KO GPMVs at basal level

Sample	Mean GP Value	SD	N
WT	-0.5196	0.05578	4997
R1KO	-0.5994	0.05272	4995
R2KO	-0.6065	0.04453	4999
R2R1KO	-0.598	0.04409	4994

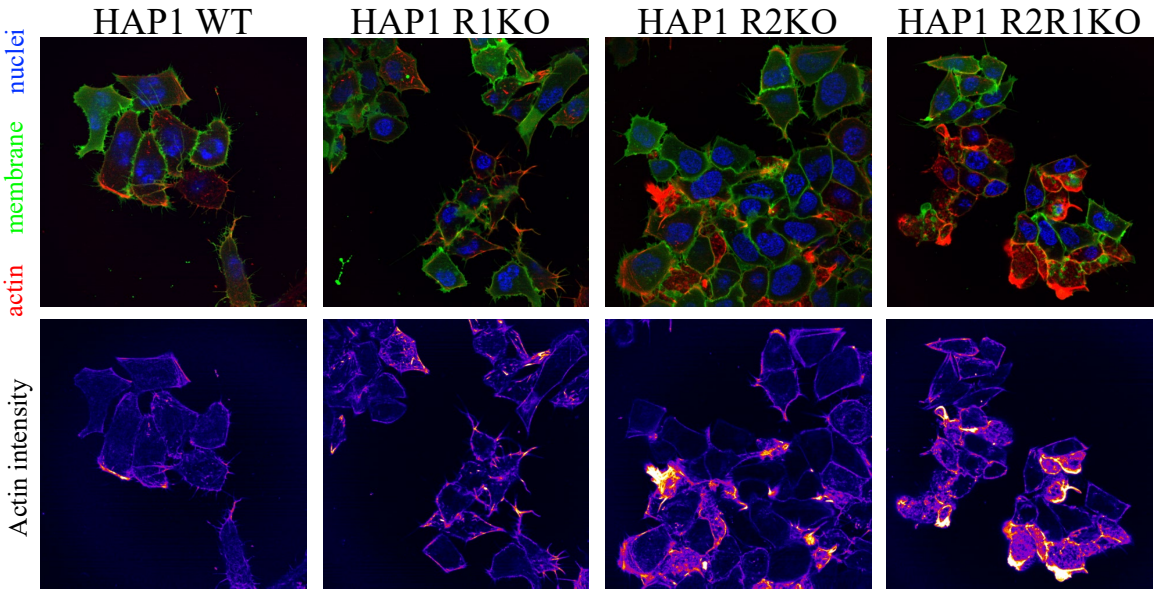

Figure S5. HAP1 whole cell confocal imaging comparing the effect of AdipoR knockout on actin polymerization. Representative confocal image of HAP1 cells stained with CellMask Green Plasma Membrane Stain, SiR-actin, and Hoechst 3342 trihydrochloride. Green plasma membrane stain was used to outline the cells and determine regions of interest.

Table S6. HAP1 whole cell confocal imaging comparing the effect of AdipoR knockout on actin polymerization. Raw intensity values of HAP1 WT, R1KO, R2KO, R2R1KO actin polymerization

Sample	Mean Intensity	SD	N
WT	21.11	11.58	136
R1KO	19.95	13.34	302
R2KO	22.97	8	226
R2R1KO	33.25	20.69	217

Table S7. Free cholesterol decreases in the absence of adiponectin receptor 2. (A) Raw values obtained by phosphate colorimetric assay for four cell lines. (B) Raw values of total cholesterol obtained by amplex red cholesterol assay for four cell lines. (C) Raw values of free cholesterol obtained by amplex red cholesterol assay for four cell lines. Cholesterol concentration was normalized to the phospholipid concentration using an inorganic phosphate assay.

A

Phosphate std	Absorbance	**Samples**	Absorbance
0 nmol	0.086	WT	0.345
0.2 nmol	0.161	R1KO	0.282
0.4 nmol	0.231	R2KO	0.4365
0.6 nmol	0.337	DKO	0.307
0.8 nmol	0.431		
1 nmol	0.506		
2 nmol	0.947		
3 nmol	1.342		
4 nmol	1.702		
5 nmol	1.966		

B

Chol std	Absorbance	**Sample**	Absorbance
0 ug/mL	1709.887	WT	37878.99
0.5 ug/mL	4381.422	R1KO	31093.885
1 ug/mL	8029.594	R2KO	32480.44
2 ug/mL	14266.391	DKO	36551.17
4 ug/mL	24978.097		
8 ug/mL	39903.84		
16 ug/mL	56167.737		

C

Chol std	Absorbance	**Sample**	Absorbance
0 ug/mL	1679.883	WT	37285.64
0.5 ug/mL	4150.629	R1KO	30868.15
1 ug/mL	7662.325	R2KO	32890.36
2 ug/mL	13775.722	DKO	36535.06
4 ug/mL	24246.258		
8 ug/mL	38857.149		
16 ug/mL	55115.873		